

W. E. Nagel · D. B. Kröner
M. M. Resch *Editors*

High Performance Computing in Science and Engineering '08



H L R I S

 Springer

High Performance Computing in Science
and Engineering '08

Wolfgang E. Nagel · Dietmar B. Kröner ·
Michael M. Resch
Editors

High Performance Computing in Science and Engineering '08

Transactions of the High Performance Computing Center
Stuttgart (HLRS) 2008

 Springer

Wolfgang E. Nagel
Zentrum für Informationsdienste
und Hochleistungsrechnen (ZIH)
Technische Universität Dresden
Helmholtzstr. 10
01069 Dresden
wolfgang.nagel@tu-dresden.de

Dietmar B. Kröner
Abteilung für Angewandte Mathematik
Universität Freiburg
Hermann-Herder-Str. 10
79104 Freiburg, Germany
dietmar@mathematik.uni-freiburg.de

Michael M. Resch
Höchstleistungsrechenzentrum
Stuttgart (HLRS)
Universität Stuttgart
Nobelstraße 19
70569 Stuttgart, Germany
resch@hlrs.de

Front cover figure: 3D-flame-modeling for industrial combustion equipment: Computed oxygen concentration in the furnace of a 330 MWe coal fired power plant (RECOM Services GmbH; www.recom-services.de)

ISBN 978-3-540-88301-2

e-ISBN 978-3-540-88303-6

DOI 10.1007/978-3-540-88303-6

Library of Congress Control Number: 2008936098

Mathematics Subject Classification (2000): 65Cxx, 65C99, 68U20

© 2009 Springer-Verlag Berlin Heidelberg

This work is subject to copyright. All rights are reserved, whether the whole or part of the material is concerned, specifically the rights of translation, reprinting, reuse of illustrations, recitation, broadcasting, reproduction on microfilm or in any other way, and storage in data banks. Duplication of this publication or parts thereof is permitted only under the provisions of the German Copyright Law of September 9, 1965, in its current version, and permission for use must always be obtained from Springer. Violations are liable for prosecution under the German Copyright Law.

The use of general descriptive names, registered names, trademarks, etc. in this publication does not imply, even in the absence of a specific statement, that such names are exempt from the relevant protective laws and regulations and therefore free for general use.

Cover design: WMXDesign, Heidelberg

Printed on acid-free paper

987654321

springer.com

Overview on the HLRS- and SSC-Projects in the Field of Transport and Climate	
<i>Ch. Kottmeier</i>	441
Effects of Intentional and Inadvertent Hygroscopic Cloud Seeding	
<i>H. Noppel and K.D. Beheng</i>	443
The Agulhas System as a Key Region of the Global Oceanic Circulation	
<i>A. Biastoch, C.W. Böning, M. Scheinert, and J.R.E. Lutjeharms</i>	459
HLRS Project Report 2007/2008: "Simulating El Nino in an Eddy-Resolving Coupled Ocean-Ecosystem Model"	
<i>U. Löptien and C. Eden</i>	471
Structural Mechanics	
<i>P. Wriggers</i>	479
Numerical Studies on the Influence of Thickness on the Residual Stress Development During Shot Peening	
<i>M. Zimmermann, M. Klemenz, V. Schulze, and D. Löhe</i>	481
A Transient Investigation of Multi-Layered Welds at Large Structures	
<i>T. Loose</i>	493
High Performance Computing and Discrete Dislocation Dynamics: Plasticity of Micrometer Sized Specimens	
<i>D. Weygand, J. Senger, C. Motz, W. Augustin, V. Heuveline, and P. Gumbsch</i>	507
Miscellaneous Topics	
<i>W. Schröder</i>	525
Molecular Modeling of Hydrogen Bonding Fluids: New Cyclohexanol Model and Transport Properties of Short Monohydric Alcohols	
<i>T. Merker, G. Guevara-Carrión, J. Vrabec, and H. Hasse</i>	529
Investigation of Process-Specific Size Effects by 3D-FE-Simulations	
<i>H. Autenrieth, M. Weber, V. Schulze, and P. Gumbsch</i>	543
Andean Orogeny and Plate Generation	
<i>U. Walzer, R. Hendel, C. Köstler, and J. Kley</i>	559
Hybrid Code Development for the Numerical Simulation of Instationary Magnetoplasmadynamic Thrusters	
<i>M. Fertig, D. Petkow, T. Stindl, M. Auweter-Kurtz, M. Quandt, C.-D. Munz, J. Neudorfer, S. Roller, D. D'Andrea, and R. Schneider</i> ..	585
Doing IO with MPI and Benchmarking It with SKaMPI-5	
<i>J. Mathes, A. Perogiannakis, and T. Worsch</i>	599

A Transient Investigation of Multi-Layered Welds at Large Structures

Tobias Loose

Ingenieurbüro Tobias Loose GbR, Haid-und-Neu-Straße 7, D-76131 Karlsruhe
loose@tl-ing.de

1 Introduction

Since welding processes are developed and used welding distortions have been known as well. The distortions influence the dimensional accuracy of the welded construction and the remaining residual stresses can effect the load carrying capacity and the stiffness of a member negatively. Therefore, residual stresses, welding distortions and their mitigation are the focus of many projects.

In the last few years growing calculation capacity enables a welding simulation of small welds on conventional PCs. Powerful parallel computing stations e.g. the HP-XC4000 of the Rechenzentrum of the Universität Karlsruhe which was launched in 2007 permit a transient welding simulation of members for in civil engineering common dimensions.

One interesting question in welding engineering is the different behavior of single- and multi-layered welds. With the powerful utility of supercomputing residual stresses and distortions of the mentioned members and their influence can be investigated.

The investigation of this question was performed using the geometry of a cylinder segment which is welded circumferentially. The chosen dimensions are a radius R of 6000 mm, a sheet thickness $t = 6$ mm and a cylinder segment of 11,25; the chosen cylinder segment has an arc length of 1178 mm.

The numerical model is using a combination of shell and volume elements. The welded area with its highly non linear behavior with high gradients across the thickness is represented by a fine mesh of volume elements and the boundary areas with shell elements.

Although the model uses a lot tolerable simplifications a mesh with a high value of nodes and elements is needed.

The finite-element calculations are performed on the HP-XC4000 using the program SYSWELD from the ESI Company. The simulations include phase transformations of steels and the resulting important effects.

2 Heat Sources for Two-Layered Welds

The two-layered welds are investigated for two different kind of joints, a V-butt joint and a X-butt joint. The first layer is welded from inside of the cylinder.

To point out the difference between single- and multi-layered welds, the V-butt and X-butt joint is modelled as a single joint with backing run as well. The criterion for the chosen parameters for the single joint with the backing run is the creation of a weld bead similar to the weld beads of the conventional V-butt and X-butt joint. The temperature distribution in the cross-section of the investigated two-layered welds can be seen in figure 1.

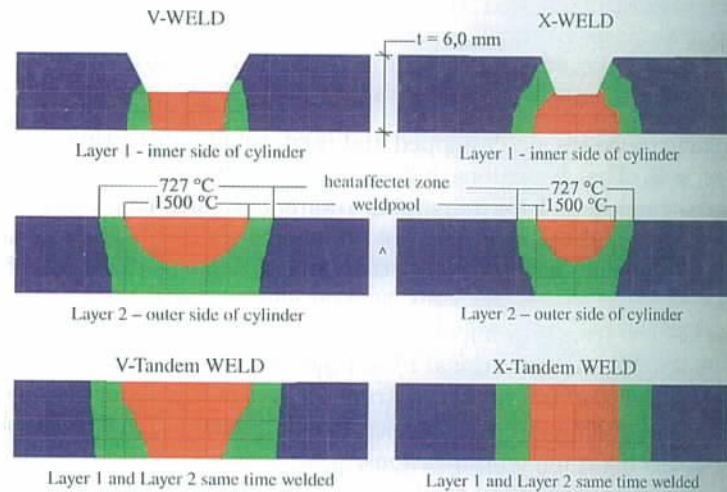


Fig. 1. Temperature distributions of the two-layered welds

3 Overview of the Investigated Cases

Using shell-volume-element models, cylinders made of the steel grade S355 and with the dimensions listed in table 1 are used. The temperature fields due to the different welding orders are varied. The cylinder slenderness $\frac{R}{t}$ is 1000. The expected critical stresses are elastic stresses.

Table 1. Dimensions and welding orders of the invested cases

Material	R	t	Segment	L	Tacks	Welding order
	mm	mm		mm		1th layer - 2nd layer
S355	6000	6	11,25	2400	5	4 - 2

The tack welds are made with five equidistant tackings with 1 cm length each. The distance between tackings is 295 mm. Only the first inner layer is tacked. The tack welds start at 0 s.

Two geometries of a weld line are investigated: X-butt joint and V-butt joint. The welding gap is filled from alternating sides in case of the chosen X-butt joint. This causes a nearly symmetrical heat input. Therefore, this case is similar to the single-layer joint of the previous chapter, the only difference is a reheating of the start and the end of previously welded layers. The filling of the welding gap in case of a V-butt joint is one-sided and unsymmetrical. The angular distortion known from V-butt joint of plates leads in case of a perimeter weld line on a cylinder and for the desired opening of the welding gap outwards to an enlargement of radial deformation inwards. The chosen forms of joints describe favorable and inappropriate orders of weld line geometries referring to the distortions.

The first layer - in case of a multi-layered joint - is welded following welding order 4, the second layer with welding order 2. Welding line 2 of the first layer starts at 1000 s, welding line 1 of the first layer starts at 2000 s and the welding line of the second layer at 3000 s.

In models with single-layered weld line the welding order 4 is used with in previous paragraph mentioned times for layer 1. The heat source in single-layer models is modelled in the way, that the melting pool of a single layer joint equates to molten area of a multi-layer joint.

Proper parameters of the investigated models are shown in table 2.

Table 2. Weldform realisations of the investigated cases

Cylinder Name	Weld
V2	two-layered V-weld
V1	single-layered V-weld
X2	two-layered X-weld
X1	single-layered X-weld

4 Axial Stresses

For the model with a double-layer welded V-butt joint (V2) the axial stresses at the equator in the middle of the shell after tacking, after the welding of the first layer and after the welding of the second layer are shown in picture 2.

An axial stress bulb known from single-layer welded cylinders occurs after the layer 1 between the weld joint 1 and 2. This is visible in the middle of the segment where there is a tensile-compression-stress-change of the blue curve in picture 2.

The compression stresses prevailing in this curve are a result of the eccentricity of the middle area of the shell in case that, after layer 1, the welding gap is filled only to a half.

Axial residual stresses disappear after the overwelding of butt joint change from layer 1 to layer 2. this is shown with the green curve in picture 2.

The situation respected to axial stresses for X-butt joint is the same as for V-butt joints.

In case of a X-butt joint the situation referable to axial stresses equals to the situation in case of a V-butt joint.

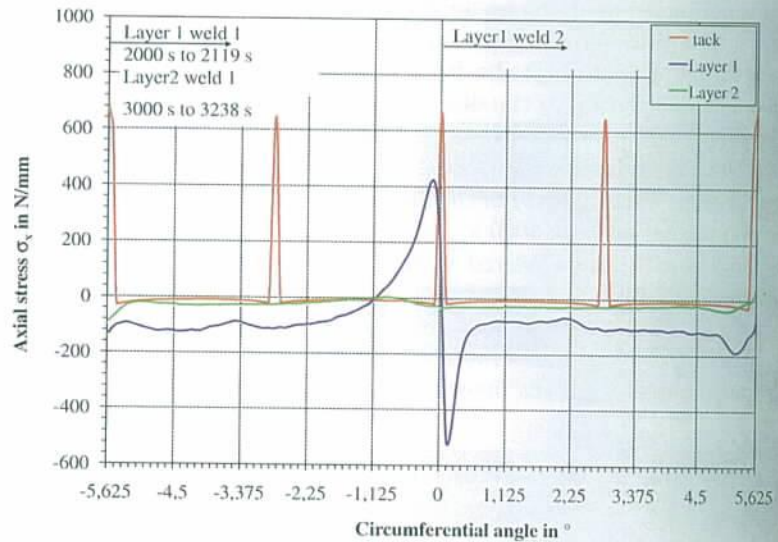


Fig. 2. Axial stress σ_x in $\frac{N}{mm^2}$ at the equator of the shell midth, two-layered v-butt joint (V2)

5 Welding Distortions

The highest radial deformations w outwards and inwards for the investigated models are arranged in table 3. Deformations normalized to the section thickness are presented in table 4. The highest radial deformations inwards are located - as well as in cases of single-layer weld lines - in the weld line adjacent area.

Picture 3 shows the radial deformation w after separate steps for cases with X-butt weld (X1, X2) at the meridian $VL = -2,8125$. The weld line 2 is on the right side of the segment and not on the examined Meridian. This is the reason why the deformation in the middle of the second weld line is oriented outwards.

The inwards oriented radial deformation of the two-layer welded cylinder segment is significant lower than in case of a single-layer welded segments. This is visible in picture 3 for a X-butt weld and is also valid for a V-butt weld (table 3).

Table 3. Maximum values of the radial deformation w in mm

Weld	V 2-layered	V 1-layered	X 2-layered	X 1-layered
after Tacking:				
outwards	0,314	0,314	0,314	0,314
inwards	0,0672	0,0672	0,0672	0,0672
after Layer 1:				
outwards	0,479	-	0,379	-
inwards	0,682	-	0,841	-
after Layer 2:				
outwards	0,170	0,273	0,136	0,257
inwards	1,611	2,00	1,24	1,95

In the picture 4 we can see the radial deformation at the equator for a double-layer V-butt weld and in picture 5 for a double-layer X-butt-weld after single process steps.

The second layer of the V-butt weld has a clearly larger volume of the molten pool than the second layer of the X-butt weld. This is the reason for a much larger weldseam shrinkage compared to a model using X-butt weld.

Welding deformations are demonstrated in pictures 4 to 4 for investigated models.

Table 4. Maximum values of the normalized radial deformation $\frac{w}{t}$

Weld	V 2-layered	V 1-layered	X 2-layered	X 1-layered
after Tacking:				
outwards	0,0523	0,0523	0,0523	0,0523
inwards	0,0112	0,0112	0,0112	0,0112
after Layer 1:				
outwards	0,0798	-	0,0632	-
inwards	0,114	-	0,140	-
after Layer 2:				
outwards	0,0283	0,0455	0,0227	0,0428
inwards	0,269	0,333	0,207	0,325

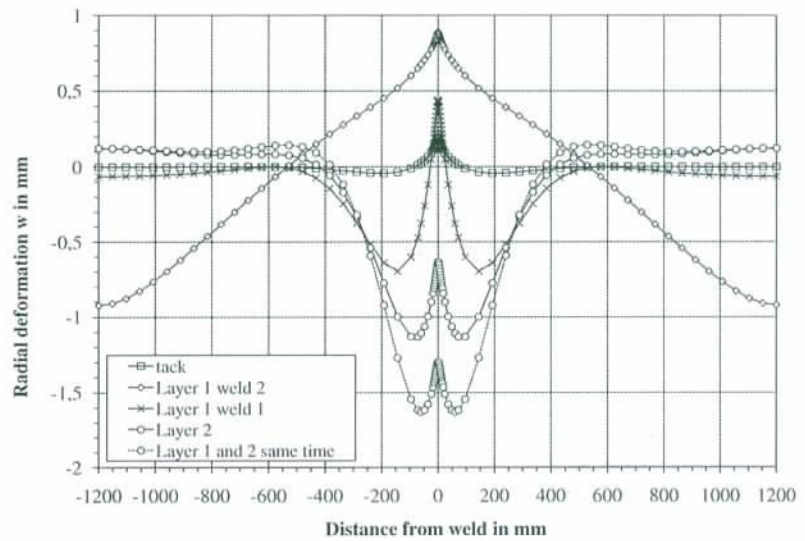


Fig. 3. Radial deformation w in mm at the meridian $VL = -2,8125$, two-layered (X2) and single-layered (X1) X-butt weld

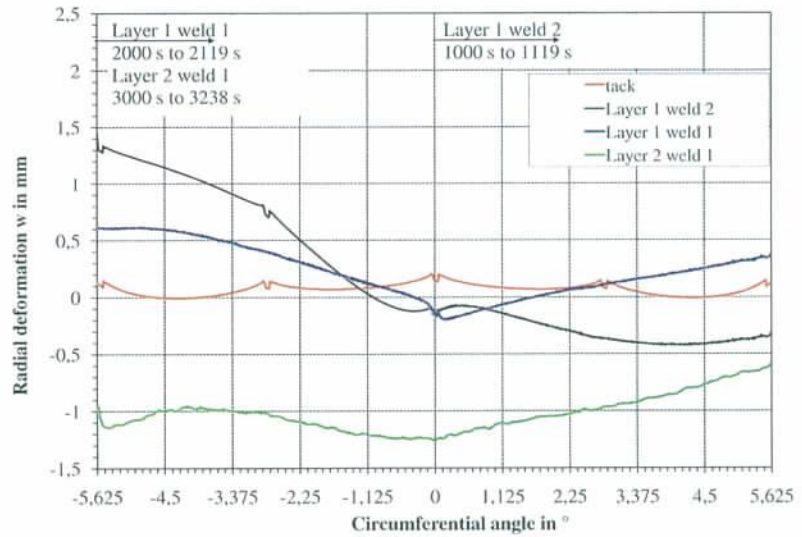


Fig. 4. Radial deformation w in mm at the equator, two-layered V-butt weld (V2)

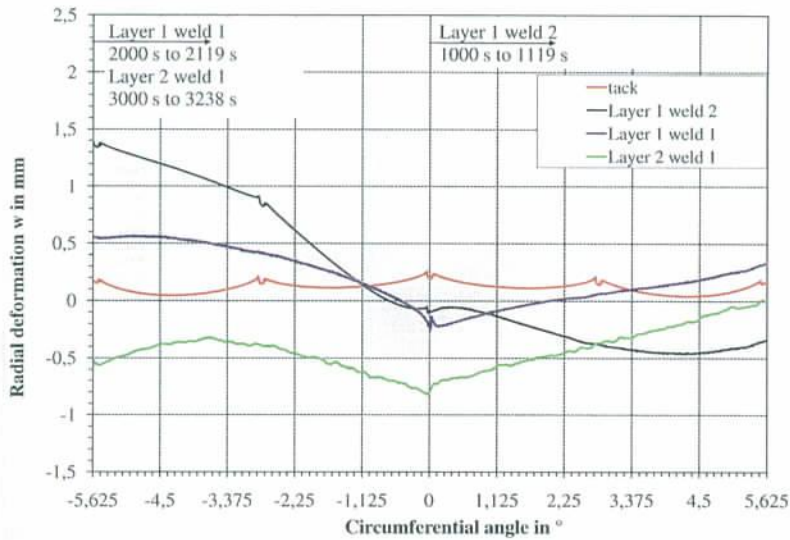


Fig. 5. Radial deformation w in mm at the equator, two-layered X-butt weld (X2)

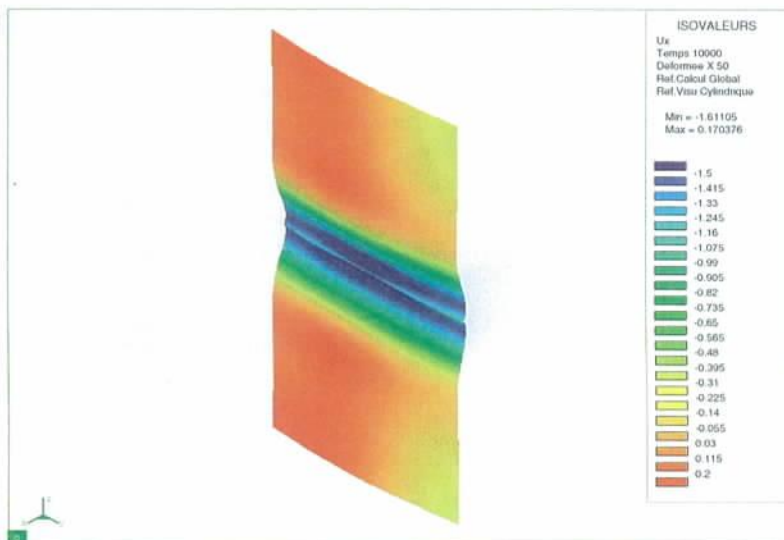


Fig. 6. Radial deformation w in mm after welding, 50-times deformed, two-layered V-butt weld (V2)

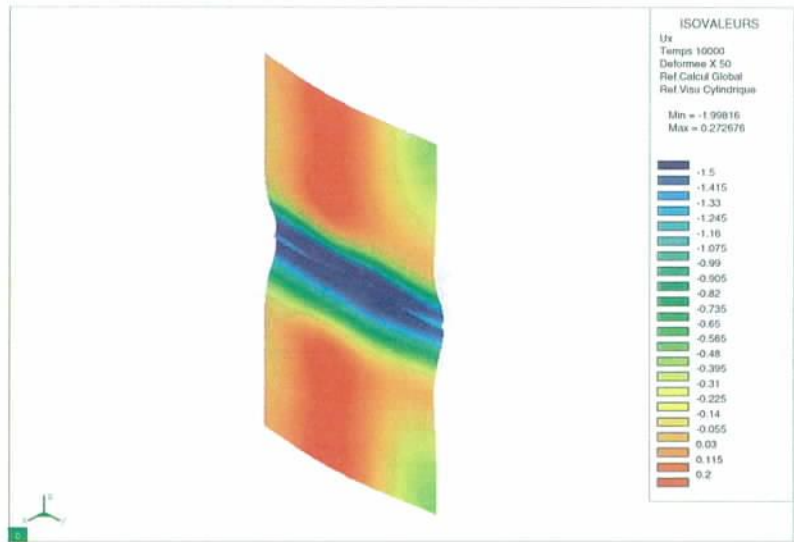


Fig. 7. Radial deformation w in mm after welding, 50-times deformed, single-layered V-butt weld (V1)

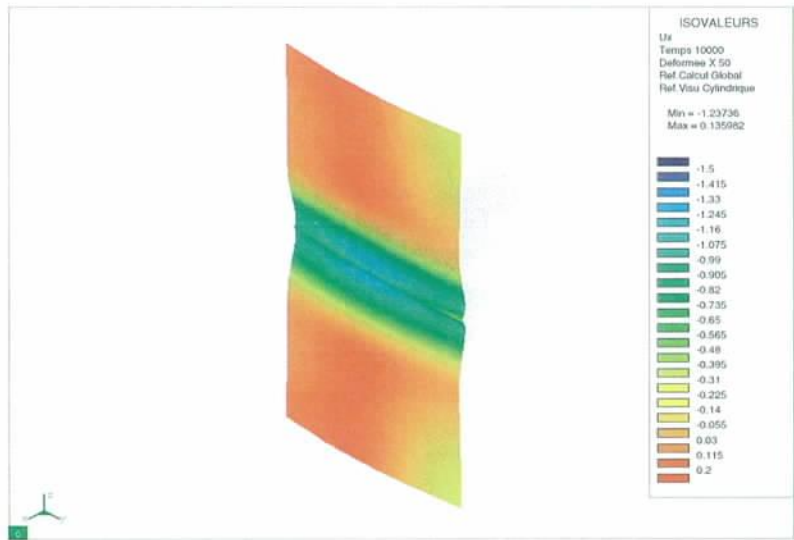


Fig. 8. Radial deformation w in mm after welding, 50-times deformed, two-layered X-butt weld (X2)

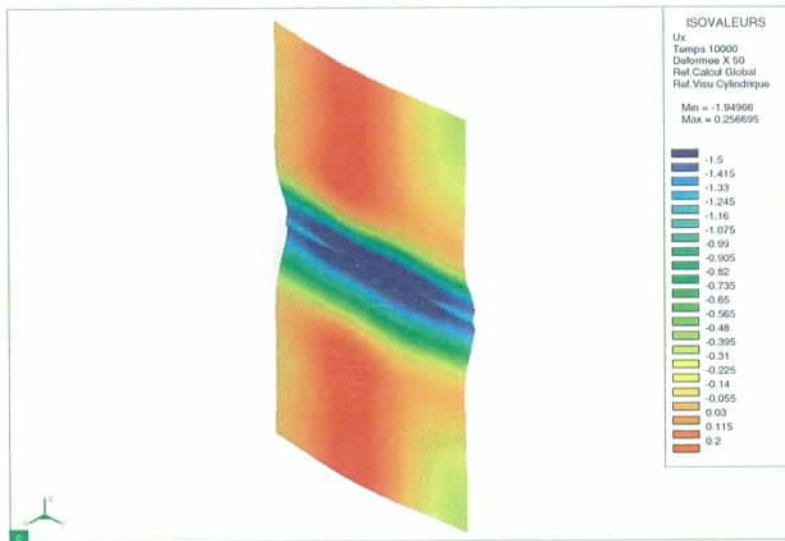


Fig. 9. Radial deformation w in mm after welding, 50-times deformed, single-layered X-butt weld (X1)

6 Critical Stresses Under Axial Load

Critical stresses under axial load of investigated models are described in table 5. Deformations belonging to the critical stresses are shown in pictures 10 to 13.

Calculated critical stresses are larger compared to models with single-layer weld line and comparable slenderness of the cylinder, which is a result of the chosen size of a segment, which is 11,25 and very small. This causes a high perimeter spindle count and a high eigenvalue. For this reason, the critical stresses are only to be considered as comparative values of different models.

Critical stresses in models with single-layer butt welds and double-layer V-butt weld are in the same order of magnitude. The critical stress in case of a double-layer X-Butt weld is significant larger. The reason for this effect is a much smaller radial deformation in this model.

Table 5. Critical stress σ_{gr} in $\frac{N}{mm^2}$

Cylinder Name	Weld	critical stress	normed critical stress $\frac{\sigma_{gr}}{\sigma_{kl}}$
V2	V 2-layered	84,5	0,67
V1	V 1-layered	86,6	0,68
X2	X 2-layered	99,7	0,79
X1	X 1-layered	86,5	0,68

The clearly reduced distortion in case of the two-layers X-butt weld compared to a single-layer welding causes a significant augmentation of critical stresses. It can be stated for this welding geometry, that a simplified calculation of single-layer welding is a conservative estimation.

The difference of distortion between a double-I V-butt weld and a single-layer V-butt weld is less distinctive than in case of an X-butt weld. The buckling is however clearly different. The buckling at the beginning and the end of the weld line in the middle of the segment is more developed. In case of a two-layers weld line lies the distinctive buckling at the left border of the segment. This is the reason for the following conclusion:

There are significant geometrical and structural imperfections in the transition area begin of the welding line - end of the welding line that are leading to a distinctive buckling in ultimate state. This is shown in models with single-layer perimeter weld line as well as the model with a single-layer V-butt weld (Picture 11). If, in case of a multi-layer weld line, the beginning and the end areas of the weld line are overwelded, the imperfections of the first layer are diminished, the buckling takes effect in some other area, in investigated model (Picture 10) on the left border of the segment.

The calculated critical stresses are equal in both models with a V-Butt weld. It can be observed that the simplified calculation with a single-layer weld line leads to equal critical stresses as a multi-layered calculation.

We can conclude that multi-layered welding does not lead to larger imperfections compared to a single-layered welding. The results of a parametric study with single-layered welding can be transferred to cylinders with greater sheet thickness that are welded multi-layered for reasons of production technology.

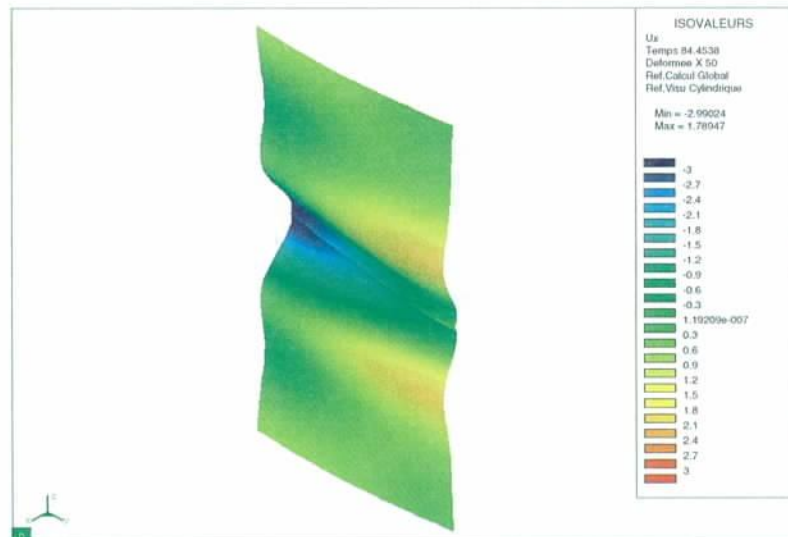


Fig. 10. Radial deformation w in mm under critical load, 50-times deformed, two-layered V-butt weld (V2)

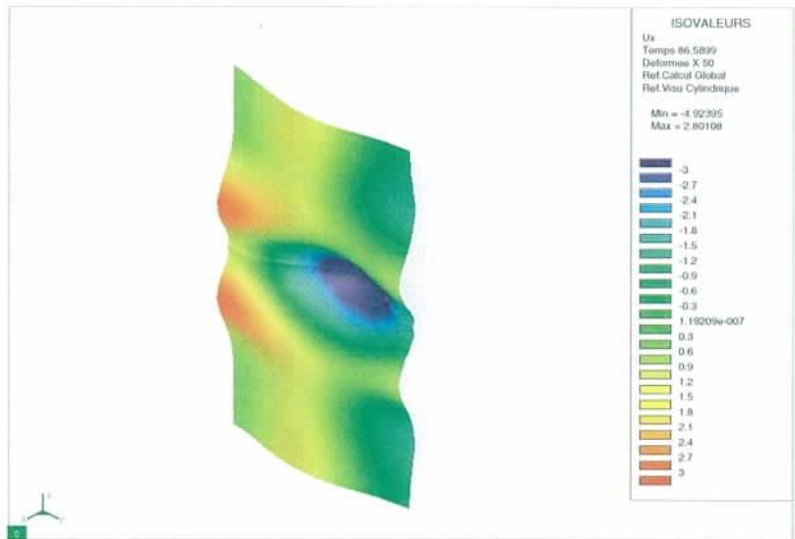


Fig. 11. Radial deformation w in mm under critical load, 50-times deformed, single-layered V-butt weld (V1)

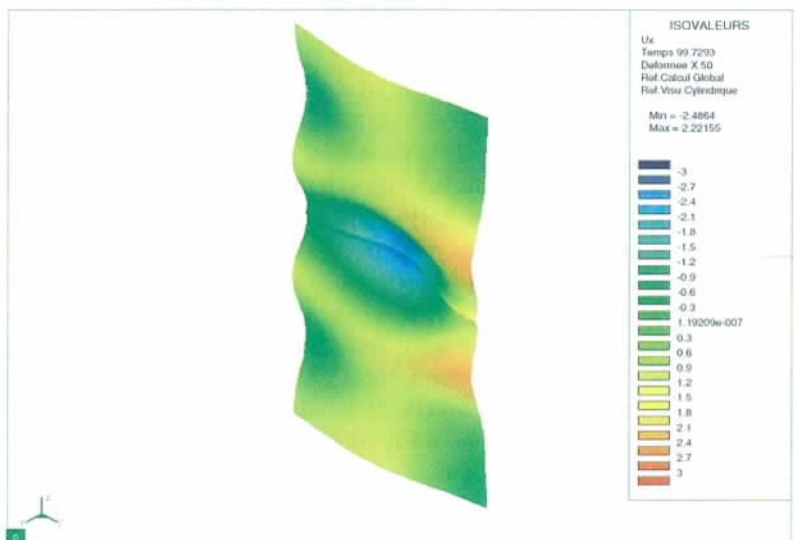


Fig. 12. Radial deformation w in mm under critical load, 50-times deformed, two-layered X-butt weld (X2)

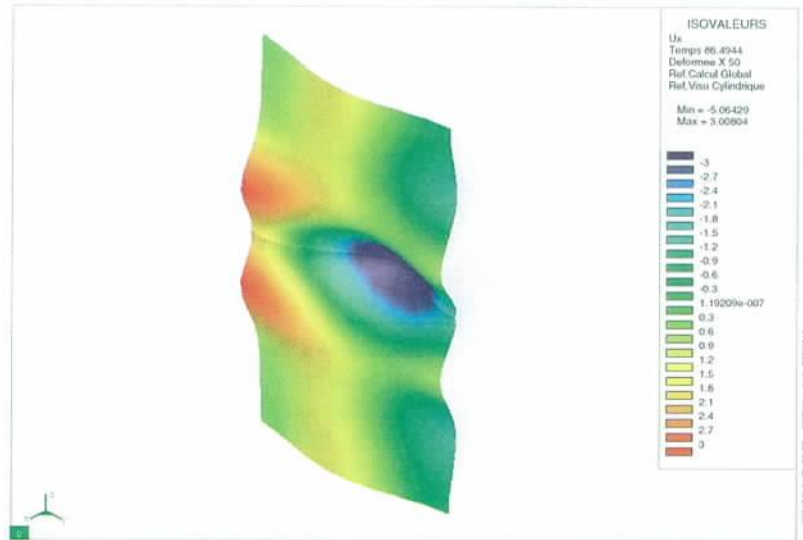


Fig. 13. Radial deformation w in mm under critical load, 50-times deformed, single-layered V-butt weld (V1)

7 Calculation Times

A particular difficulty of the welding simulation lies in the calculation of large gradients that appear during the calculation of the temperature field as well as in the mechanical calculation. It is necessary to use a fine mesh in the weld line area and small time steps during the calculation of welding. This causes a high calculation complexity for finite elements models.

The calculations of multi-layered weld lines were made at scientific super-computer HP XC4000 at the electronic data processing center of the Universität Karlsruhe.

The calculations using Sysweld were done - depending of the certain model - on a node with 4 CPUs. A calculation duration of one day results in a needed calculation complexity of 4 CPU-days. It is allowed to start up to 10 calculations per user simultaneous, so the models for the parametric study were calculated at the same time. Because of a long calculation duration for one model a huge time saving compared to a total calculation time for all models was reached.

Geometry, mesh size, welding time and the calculation times divided in the calculation of the temperature field, mechanical calculations and the calculation of axial critical stresses for a Shell-Volume-Model with a double-layer weld line are shown in the table 6.

Table 6. Calculation time for a shell-volume model of a cylinder segment with multi-layered circumferential welds

Cylindername	V2
R in mm	6000
t in mm	6
L in mm	2400
Segment in degrees	11,25
Segment in mm	1178
Area in m ²	2,83
Number of nodes	77 823
Number of shellelements	12 288
Number of volumeelements	55 296
Welding time in s	474
Thermal analysis:	
Number of timesteps	710
Computingtime in days	1,45
Computingtime in CPU-days	5,82
Mechanical analysis:	
Number of timesteps	859
Computingtime in days	25,2
Computingtime in CPU-days	101
calculation of the axial critical stress:	
Number of timesteps	51
Computingtime in days	0,35
Computingtime in CPU-days	1,41